Vision Research 127 (2016) 132–140

Contents lists available at ScienceDirect

Vision Research

journal homepage: www.elsevier.com/locate/visres

Contour integration with corners

Malte Persike *, Günter Meinhardt

Psychological Institute, Department of Statistical Methods, Johannes Gutenberg University Mainz, Wallstr. 3, D-55122 Mainz, Germany

ARTICLE INFO

Article history:
Received 19 March 2016
Received in revised form 11 June 2016
Accepted 4 July 2016
Available online 31 August 2016

Keywords:
Contour integration
Corners
Psychophysics
Spatial vision
Humans

ABSTRACT

Contour integration refers to the ability of the visual system to bind disjoint local elements into coherent global shapes. In cluttered images containing randomly oriented elements a contour becomes salient when its elements are coaligned with a smooth global trajectory, as described by the Gestalt law of good continuation. Abrupt changes of curvature strongly diminish contour salience. Here we show that by inserting local corner elements at points of angular discontinuity, a jagged contour becomes as salient as a straight one. We report results from detection experiments for contours with and without corner elements which indicate their psychophysical equivalence. This presents a challenge to the notion that contour integration mostly relies on local interactions between neurons tuned to single orientations, and suggests that a site where single orientations and more complex local features are combined constitutes the early basis of contour and 2D shape processing.

1. Introduction

When looking at a visual scene, conditions are rarely ideal for building an intact representation of the objects it contains and the relations among them. One of the obstacles for the visual system is the partial occlusion of object boundaries, turning a contiguous edge into an assembly of perceptually disjoint segments with similar orientation (Geisler & Perry, 2009). The term contour integration commonly refers to the ability of the visual system to bind such spatially distributed local elements into a complete percept (Hess & Field, 1999). The integration of visual contours can operate on many different visual properties, yet the most prominent variant involves the orientation of local elements. Its two necessary conditions are for (a) the elements to fall on a smooth spatial trajectory and (b) their orientations to coalign with the curvature of that trajectory (Hess & Dakin, 1997). Whenever contour curvature is too jagged and inflections along the global trajectory become too sharp, contour visibility decreases down to the point where contour integration ceases entirely (Pettet, 1999). The same holds true whenever the orientation of local elements deviates too much from global curvature (Persike & Meinhardt, 2015).

These characteristics have been elegantly captured by the association field model (Field, Hayes, & Hess, 1993). The association field operates on collinear orientations of disjoint local stimulus elements and allows to integrate them into a contiguous contour percept. The human visual system has developed specialized patterns of neural connectivity to achieve this binding of local elements based on their orientation (Kovacs, 2000; Kiorpes & Bassin, 2003; Baker, Tse, Gerhardstein, & Adler, 2008). Research has suggested that interconnections between orientation detectors may indeed be the neural basis of contour integration (Hess & Field, 1999). Lateral connections in the form of inter-columnar synaptic fibers have been found, among others, in the macaque (Malach, Amir, Harel, & Grinvald, 1993; Kapadia, Westheimer, & Gilbert, 2000) and the cat (Schmidt, Goebel, Lowel, & Singer, 1997). Even in early layers of visual cortex, lateral connections span preferentially between neurons with similar preferred orientations (Stettler, Das, Bennett, & Gilbert, 2002; Ng, Bharath, & Zhaoping, 2007) although the correspondence between the spatial characteristics of horizontal projections and contour perception is disputable (Li & Gilbert, 2002).

Most formulations of the association field model have the binding strength between neighboring elements depend on their orientation collinearity (Yen & Finkel, 1998; Li, 1998; Papari & Petkov, 2011). The smoother a trajectory and the better its local elements coalign, the more salient a contour becomes. This notion has received overwhelming empirical support (see Hess, Hayes, & Field, 2003 for an overview), yet it rests on one important presupposition: the individual contour elements are set to be "mono-oriented", meaning that they carry only one orientation component. This poses a decisive constraint given that research

* Corresponding author.
E-mail addresses: persike@uni-mainz.de (M. Persike), meinharg@uni-mainz.de (G. Meinhardt).

http://dx.doi.org/10.1016/j.visres.2016.07.010
0042-6989/© 2016 Published by Elsevier Ltd.

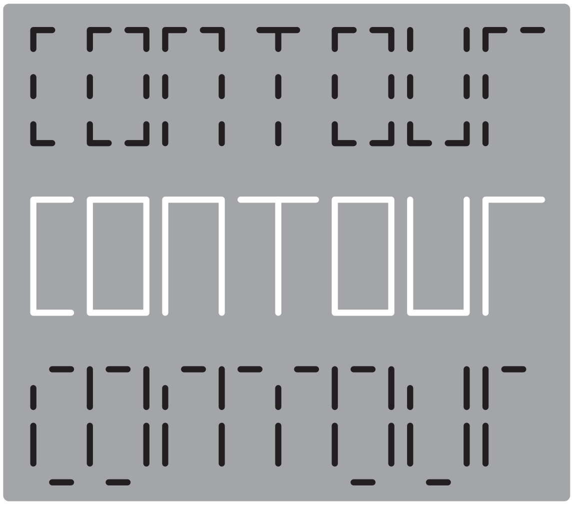

Fig. 1. The effect of corners in contour integration. Both segmented variants of the word "contour" fit perfectly into the solid reference printed in the middle. Although the total length of line segments is identical for the corresponding letters of each word, the upper instance with corner elements remains perfectly legible while the bottom version with only straight segments is unreadable.

has emphasized the pivotal role of corners and junctions for the processing of object shape (Marr, 1980). When humans view the outline of an object, the deletion of corners or junctions significantly impedes the perception of said object (Shevelev, Kamenkovich, & Sharaev, 2003). By contrast, as long as only straight parts of the outline are deleted, recognizability is largely retained (see Fig. 1). Information theory posits that shape information is not distributed uniformly along a contour but concentrated in regions of high curvature or pure angular discontinuity (Attneave, 1954; Feldman & Singh, 2005) which have moreover been shown to be perceptually equivalent (Landy & Bergen, 1991). If present along object outlines, corners are such points of angular discontinuity where the continuation of a contour can no longer be predicted easily from its previous course. With their capacity to encode local image complexity (Rodrigues & du Buf, 2006), corners thus serve as salient cues for global shape analysis (Kristjansson & Tse, 2001) and visual scene representations (Biederman, 1987).

The predominant stimulus configuration used in contour integration research is devoid of visible corners. Contours are generally created from collinear local band-pass elements, embedded in fields of similar elements with random orientation (Field et al., 1993). Hence, in contour integration research, the concept of corners (Bowden, Dickinson, Fox, & Badcock, 2015) or turning points (Mathes & Fahle, 2007) always refers to the invisible global trajectory of a contour, not the visible local elements it is made of. Whenever high magnitudes of curvature occur along such contours, contour shape becomes more complex and contours loose saliency (Wilder, Feldman, & Singh, 2015a, 2015). In terms of association field models, the two elements adjacent to a point of angular discontinuity must necessarily exhibit different orientations which has proven detrimental to contour visibility (Hess & Dakin, 1997; Pettet, 1999). It is straightforward to ask whether the decline in visibility for contours with sharp inflections along their trajectory can be remedied by the insertion of corner elements at the points of angular discontinuity.

In the series of experiments described here, we examine the role of corner elements in contour integration. Moreover, we seek to discern whether a common neural process might be responsible for the integration of contours with and without corners.

2. Methods

2.1. Stimuli

Stimuli were constructed from Gabor micropatterns. The mono-oriented variant with only one orientation component is defined by

$$g(x,y) = \exp\left(-\frac{x^2+y^2}{2\sigma^2}\right)\sin\left(2\pi f\left(x\cos\left(\frac{\varphi}{180}\pi\right) - y\sin\left(\frac{\varphi}{180}\pi\right)\right)\right). \quad (1)$$

We further defined circular sines as

$$g(x,y) = \exp\left(-\frac{x^2+y^2}{2\sigma^2}\right)\sin\left(2\pi f\sqrt{x^2+y^2}\right), \quad (2)$$

and Gaussian blobs according to

$$g(x,y) = \exp\left(-\frac{x^2+y^2}{2\sigma^2}\right). \quad (3)$$

Carrier spatial frequency of Gabors and circular sines was fixed at $f = 3.25$ cycles per degree visual angle in all experiments but one. Variations are described in the respective experimental section. The Gaussian hull had a standard deviation of $\sigma = 0.24^\circ$ visual angle and was clipped beyond a radius of 2.75 σ-units. Spatial phase of Gabors was set randomly to phase or counterphase sines. We also defined "corner" Gabors carrying two orientation components which differed by an angle $\pm\theta'$. Components within one patch thus touched along a boundary of $2^{-1}|\theta'|$ relative to the orientation of each.

Contours consisted of three segments, connecting at angles of alternating sign, taken from $\theta = \pm[0^\circ, 30^\circ, 50^\circ, 70^\circ, 90^\circ, \text{or } 110^\circ]$. A nonzero value of θ creates two inflection points along the contour path where segments abut (Fig. 2a). Depending on experimental condition, the segments themselves were either straight or curvilinear with a constant radius of curvature. The cardinal direction of a contour was sampled randomly from $[0^\circ \ldots 360^\circ]$. After a contour was generated and Gabors placed along its trajectory, the contour was superimposed onto a hexagonal grid of background micropatterns. The contour was always positioned within the central $10^\circ \times 10^\circ$ region of the whole $17^\circ \times 17^\circ$ stimulus area. Background elements overlapped by the contour were removed from the grid. The number of background elements thus varied slightly with an average of about 200 elements. Finally, elements were randomly displaced using a stochastic particle movement algorithm (Braun, 1999; Ernst et al., 2012). After displacement, inter-element distances of adjacent Gabor elements had a mean of about 1.34°. Orientations of background elements were sampled uniformly from the interval $[0^\circ \ldots 360^\circ]$, as were the orientations of contour elements in distracter stimuli. Contour elements in target stimuli were always perfectly collinear with the global trajectory.

2.2. Contour variants

Contours had one of three configurations (Fig. 2b). The CLASSIC condition represented the typical stimulus used in contour integration research. All elements carried a single orientation signal and points of angular discontinuity fell between two neighboring contour elements. The BRIDGE condition resembled the CLASSIC condition, only that it added two intermediate elements at the inflection points. These elements had an orientation mid-range between the orientations of the two adjacent path segments, thus bridging the orientation disparity between the two segments. Finally, in the CORNER condition, the two elements at the inflection points were corners. The orientation components of a corner element aligned perfectly with the connecting path segments. To